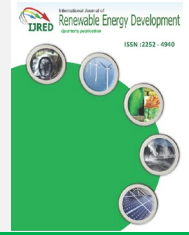




Contents list available at IJRED website

International Journal of Renewable Energy Development

Journal homepage: <https://ijred.undip.ac.id>



Research Article

Numerical Analysis of Transfer of Heat by Forced Convection in a Wavy Channel

Naseer Abboodi Madlool^a, Mohammed J. Alshukri^a, Ammar I. Alsabery^{b,*}, Adel A. Eidan^c,
Ishak Hashim^d

^aDepartment of Mechanical Engineering, Faculty of Engineering, Kufa University, 54002, Najaf, Iraq

^bRefrigeration & Air-conditioning Technical Engineering Department, College of Technical Engineering, The Islamic University, Najaf, Iraq

^cNajaf Technical College, Al-Furat Al-Awsat Technical University, 540011, Najaf, Iraq

^dDepartment of Mathematical Sciences, Faculty of Science & Technology, Universiti Kebangsaan Malaysia, 43600 UKM Bangi, Selangor, Malaysia

Abstract. Convective heat transfer of laminar forced convection in a wavy channel is studied in this paper. Numerical simulations of the 3D steady flow of Newtonian fluid and heat transfer characteristics are obtained by the finite element method. The effects of the Reynolds number ($10 \leq Re \leq 1000$), number of oscillations ($0 \leq N \leq 5$) and amplitude of the wall ($0.05 \leq A \leq 0.2$) on the heat transfer have been analyzed. The results show that the average Nusselt number is elevated as the Reynolds number is raised, showing high intensity of heat transfer, as a result of the intensified effects of the inertial and zones of recirculation close to the hot wavy wall. The rate of heat transfer increases about 0.28% with the rise of the number of oscillations. In the transfer of heat along a wavy surface, the number of oscillations and the wave amplitude are important factors. With an increment in the number of oscillations, the maximal value of the average velocity is elevated, and its minimal value occurs when the channel walls are straight. The impact of the wall amplitude on the average Nusselt number and dimensionless temperature tends to be stronger compared to the impact of the number of oscillations. An increase of the wall amplitude improves the rate of heat transfer about 0.91% when the Reynolds number is equal 100. In addition, when the Reynolds number is equal 500, the rate of heat transfer grows about 1.1% with the rising of the wall amplitude.

Keywords: Forced convection; Finite difference method; Heat transfer; Wavy channel; 3D simulation



@ The author(s). Published by CBIORE. This is an open access article under the CC BY-SA license (<http://creativecommons.org/licenses/by-sa/4.0/>).

Received: 13th July 2022; Revised: 28th Sept 2022; Accepted: 5th Nov 2022; Available online: 20th Nov 2022

1. Introduction

A strategy that is usually employed to improve the transfer of heat by convection in a channel is the application of wavy walls. The undulation disturbs the hydrodynamics as well as the thermal boundary layers, forming a recirculation zone between the undulations. The point of reattachment leads to washing of the channel wall, thereby raising the transfer of heat by convection. A number of studies have investigated how fluid and heat flow in a channel with wavy walls (cf. Alsabery *et al.* 2022; Alshukri *et al.* 2018; Bourouis and Prévost 1994; Izumi *et al.* 1983; Leontini *et al.* 2007; Nishimura *et al.* 1993; Rush *et al.* 1999; Sheikholeslami *et al.*, 2022; Wang and Vanka 1995).

The advance of computational technologies in recent years has made numerical simulation an important tool to generate results of great contribution to the engineering field, mainly in fluid mechanics and heat transfer problems (cf. Abu Talib and Hilo 2021; Eidan *et al.* 2021; Errico and Stalio 2014; Feijó *et al.* 2018; Jabbar, Alshukri, and Madlool 2018; Li *et al.* 2022; Miroshnichenko *et al.* 2017). Errico and Stalio (2014) considered a direct numerical simulation of turbulent forced convection in a wavy channel at low and order-one values of the Prandtl number (Hajjalibabaei and Saghir 2022). The numerical

simulation costs make this technique very attractive compared to the cost of high-quality experimental equipment and installations, particularly for geometrical optimization, where several different configurations need to be investigated (Adhikari *et al.* 2020). Computational techniques to complement experimental results have also proved a viable alternative to obtain reliable recommendations about design in thermal devices. Concerning specifically the investigation of corrugated or finned channels and design in channels subjected to convection heat transfer, several interesting studies have been reported. For example, Nishimura *et al.* 1989 studied convective flows in symmetric wavy-walled channels. Later, Vasudeviah and Balamurugan (2001) studied forced convective Stokes flows in a wavy channel. Afterwards, Kim *et al.* (2013) investigated the influence of different cross-sectional shapes of a printed circuit heat exchanger (PCHE) on thermal performance and pressure drop. Their results indicated that semi-circular channels gave the best performance in the multi-objective analysis. Recently, Jing *et al.* (2020) studied the hydraulic and thermal performances of laminar flow in a fractal treelike branching microchannel network with wall velocity slip. Lyu *et al.* (2020) studied the flow of fluid and transfer of heat in a microchannel

* Corresponding author

Email: ammar_e_2011@yahoo.com (A.I. Alsabery)

heat-sink using the fractal technique to define the microchannel configuration inserted in a solid with internal heat flux and considering a multiphase flow of water and kerosene. The main purpose was to achieve uniform temperature distribution in the studied domain.

Among the studies concerned with geometrical optimization in blocks mounted in channel flows, Durgam *et al.* (2017) studied the distribution of an array of heat sources under mixed convection. Authors obtained specific distances as the recommendation to improve the thermal performance. Alsabery *et al.* (2020) studied the impacts of the two-phase nanofluid approach on convection heat transfer in a 3D wavy direct absorber solar collector. Using the finite element method and particles tracking model, Alsabery *et al.* (2021) studied the forced convection heat transfer of nanofluid inside a wavy horizontal channel. Sheikholeslami (2022b) considered numerically the solar system pipe equipped with an innovative turbulator and hybrid nanofluid. A review on the applications and techniques of different channels and heat pipe-solar collector systems was performed by Alshukri *et al.* (2022). Sheikholeslami and Ebrahimpour (2022) studied the thermal improvement of a linear multi-way twisted tape Fresnel solar system containing a nanofluid. They found that convective heat transfer grows and augmentation in the interaction of fluid with the tube walls improves the friction factor. Numerical analysis of solar energy storage inside a double pipe utilizing nanofluid for the purpose of melting system was examined by Sheikholeslami (2022a). In a wavy heat sink, the heat transfer coefficient was improved by increasing the nanofluid concentrations for all given Reynolds numbers (Kumar *et al.* 2022). Mehta *et al.* (2022) found that the combined effects of heat transfer increase in a wavy channel as compared to a straight channel. Mohammadi and Shahkarami (2022) observed that by applying optimal wavy walls in the microchannel heat sink, the amount of absorbed heat increases more in pure fluid than in nanofluid.

This study numerically analyzes how the transfer of heat by forced convection in a wavy channel is affected by the Reynolds number, number of oscillations and wall amplitude. The numerical analysis used COMSOL-based finite element to solve the 3D steady problem of Newtonian fluid and thermal behavior in a wavy channel.

2. Mathematical formulation

For derivation of the equations of fluid dynamics, the primary concepts of conserving momentum, mass and energy are employed. "Equation of continuity" is the name given to the equation developed from the concept of conservation of mass. Likewise, "equation of momentum" is the name given to the equation derived from Newton's second law. Both equations are mostly sufficient to work out the flow aspect of the problems associated with fluid dynamics. There are four equations (1 continuity equation and 3 momentum equations) to find four unknown entities (3 velocity components and pressure). In addition, regarding the aspect of transfer of heat in the convection problem, a solution is needed with respect to how temperature is distributed through the flow, in particular near the solid walls that are in contact with the heat-bearing fluid stream (Al-Bonsrulah *et al.* 2021). Another equation that is needed to achieve this important goal is obtained from the first law of thermodynamics or the principle of energy conservation. "Equation of energy" is the term used to denote the equation derived by applying the concept of conservation of energy to fluid flow.

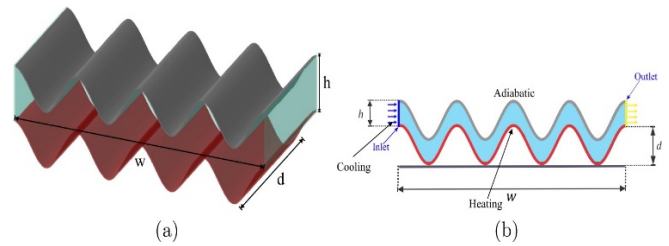


Fig 1. (a) 3D-diagrammatic representation of the physical model; (b) 2D-diagrammatic representation in the plane (X, Y)

The bottom-heated wavy channel under consideration is depicted in Fig. 1. The governing equations of the problems are

Equation of continuity:

$$\frac{\partial u}{\partial x} + \frac{\partial v}{\partial y} + \frac{\partial w}{\partial z} = 0, \tag{4}$$

Equation of momentum along x-direction:

$$u \frac{\partial u}{\partial x} + v \frac{\partial u}{\partial y} + w \frac{\partial u}{\partial z} = -\frac{1}{\rho} \frac{\partial p}{\partial x} + \nu \left(\frac{\partial^2 u}{\partial x^2} + \frac{\partial^2 u}{\partial y^2} + \frac{\partial^2 u}{\partial z^2} \right), \tag{5}$$

Equation of momentum along y-direction:

$$u \frac{\partial v}{\partial x} + v \frac{\partial v}{\partial y} + w \frac{\partial v}{\partial z} = -\frac{1}{\rho} \frac{\partial p}{\partial y} + \nu \left(\frac{\partial^2 v}{\partial x^2} + \frac{\partial^2 v}{\partial y^2} + \frac{\partial^2 v}{\partial z^2} \right), \tag{6}$$

Equation of momentum along z-direction:

$$u \frac{\partial w}{\partial x} + v \frac{\partial w}{\partial y} + w \frac{\partial w}{\partial z} = -\frac{1}{\rho} \frac{\partial p}{\partial z} + \nu \left(\frac{\partial^2 w}{\partial x^2} + \frac{\partial^2 w}{\partial y^2} + \frac{\partial^2 w}{\partial z^2} \right), \tag{7}$$

Equation of energy:

$$u \frac{\partial T}{\partial x} + v \frac{\partial T}{\partial y} + w \frac{\partial T}{\partial z} = \alpha \left(\frac{\partial^2 T}{\partial x^2} + \frac{\partial^2 T}{\partial y^2} + \frac{\partial^2 T}{\partial z^2} \right). \tag{8}$$

The boundary conditions of the above-mentioned dimensional equations are:

At the hot lower wavy surface:

$$u = 0, v = 0, T = T_h, 0 \leq x \leq W, h - A(1 - \cos(N\pi y)),$$

At the cold inlet left surface:

$$u = u_{in}, v = 0, T = T_c, x = 0, 0 \leq y \leq h,$$

At the adiabatic upper wavy surface:

$$u = 0, v = 0, \frac{\partial T}{\partial Y} = 0, 0 \leq x \leq W, d - A(1 - \cos(N\pi y)),$$

At the adiabatic outlet right surface:

$$p = 0, \frac{\partial T}{\partial x} = 0, x = W, 0 \leq y \leq h, \tag{9}$$

Introducing the dimensionless quantities:

$$X = \frac{x}{L}, Y = \frac{y}{L}, Z = \frac{z}{L}, U = \frac{u}{U_0}, V = \frac{v}{U_0}, W = \frac{w}{U_0}, \\ P = \frac{p}{\rho U_0^2}, \theta = \frac{T - T_c}{T_h - T_c}, Re = \frac{U_0}{\nu L}, Pr = \frac{\nu}{\alpha} \tag{10}$$

Upon using the similarity techniques to transform the dimensional form of equations to the dimensionless forms then yields

$$\frac{\partial U}{\partial X} + \frac{\partial V}{\partial Y} + \frac{\partial W}{\partial Z} = 0, \tag{11}$$

$$U \frac{\partial U}{\partial X} + V \frac{\partial U}{\partial Y} + W \frac{\partial U}{\partial Z} = -\frac{\partial P}{\partial X} + \frac{1}{Re} \left(\frac{\partial^2 U}{\partial X^2} + \frac{\partial^2 U}{\partial Y^2} + \frac{\partial^2 U}{\partial Z^2} \right), \tag{12}$$

$$U \frac{\partial V}{\partial X} + V \frac{\partial V}{\partial Y} + W \frac{\partial V}{\partial Z} = -\frac{\partial P}{\partial Y} + \frac{1}{Re} \left(\frac{\partial^2 V}{\partial X^2} + \frac{\partial^2 V}{\partial Y^2} + \frac{\partial^2 V}{\partial Z^2} \right), \tag{13}$$

$$U \frac{\partial W}{\partial X} + V \frac{\partial W}{\partial Y} + W \frac{\partial W}{\partial Z} = -\frac{\partial P}{\partial Z} + \frac{1}{Re} \left(\frac{\partial^2 W}{\partial X^2} + \frac{\partial^2 W}{\partial Y^2} + \frac{\partial^2 W}{\partial Z^2} \right), \tag{14}$$

$$U \frac{\partial \theta}{\partial X} + V \frac{\partial \theta}{\partial Y} + W \frac{\partial \theta}{\partial Z} = \frac{1}{Re Pr} \left(\frac{\partial^2 \theta}{\partial X^2} + \frac{\partial^2 \theta}{\partial Y^2} + \frac{\partial^2 \theta}{\partial Z^2} \right). \tag{15}$$

The rate at which heat is transferred or the Nusselt number at the bottom wavy surface is determined by the application of Fourier's law as given in Eq. (16):

$$q_w = -k \frac{dT}{dy} |_w \tag{16}$$

which then gives in dimensionless forms:

$$Nu = \frac{q_h W}{k(T_h - T_c)} = -\sqrt{\left(\frac{\partial \theta}{\partial x}\right)^2 + \left(\frac{\partial \theta}{\partial y}\right)^2 + \left(\frac{\partial \theta}{\partial z}\right)^2} |_w \tag{17}$$

The average Nusselt number at the bottom wavy surface is then obtained by integrating Eq. (21), i.e.

$$\overline{Nu} = \int_0^W Nu \, dW, \tag{18}$$

where W indicates the total length of the wavy lower heater.

3. Numerical Analysis and Validation

The dimensionless governing equations, i.e. Eqs. (11)-(15), subject to the dimensionless boundary conditions, Eq. (9), are numerically worked out based on COMSOL's PDEs (partial differential equations) solver derived from the Galerkin weighted residual finite element formulation. We have chosen to use the COMSOL finite element technique to take advantage of the capabilities of COMSOL in solving problems in complex geometries. COMSOL has ultra-modern numerical algorithms as well as tools for visualization combined with an interface that is user-friendly. With the aid of COMSOL, the laminar incompressible flow (spf) was used in Eqs. (12), (13) and (14). Also, the fluid heat transfer (ht) was used in Eq. (15).

The discretization of the computational domain to triangular elements is carried out (see Fig. 2). Triangular Lagrange finite elements associated with various orders were employed for each flow variable in the computational domain. Through substitution of the approximations in the governing equations, residuals regarding each conservation equation are achieved. For the purpose of simplification of the non-linear terms of the equation of momentum, we applied the Newton-Raphson iteration algorithm. Further, with regard to fluid flow and transfer of heat variables, segregated parametric solvers were employed. Thereafter, a PARDISO (parallel direct solver) was applied. Various grid sensitivity tests have been carried out for the purpose of finding out if the mesh scheme is adequate as well as ensuring grid-independent results. The default COMSOL settings were utilized for the predefined sizes of the mesh, that is, coarser G1, coarse G2, normal G3, fine G4, finer G5 and extra fine G6. The determined Nusselt number at diverse grid sizes are shown in Table 1 for $Re = 750$, $N = 5$ and $A = 0.1$. Grid size of G5 was selected as fine enough for resolving the flow, temperature field and local-average heat transfer.

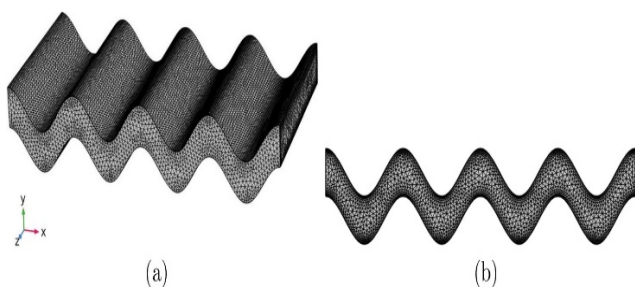


Fig 2. (a) 3D grid-points distribution for the grid-size 7625 and (b) 2D grid-points distribution for the grid-size G5.

Table 1

Grid testing regarding \overline{Nu} and pressure drop at various grid sizes with $Re = 750$, $N = 5$ and $A = 0.1$.

Grid size	Number of elements	\overline{Nu}	ΔP
G1	3934	64.362	2.8875
G2	4308	63.375	2.8889
G3	4538	62.718	2.8911
G4	4909	62.468	2.8948
G5	7625	62.418	2.8966
G6	21552	62.394	2.8981

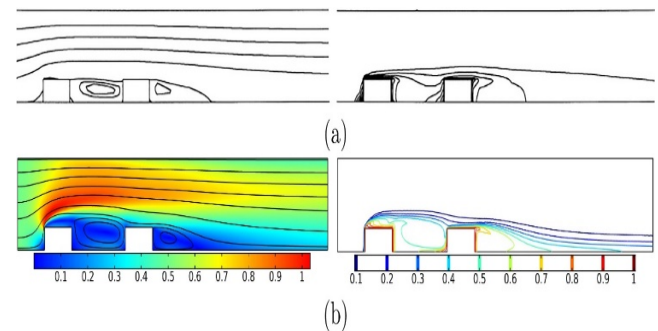


Fig 3 (a) Chen and Wang (1998); (b) current study: velocity (streamlines) - left; isotherms - right.

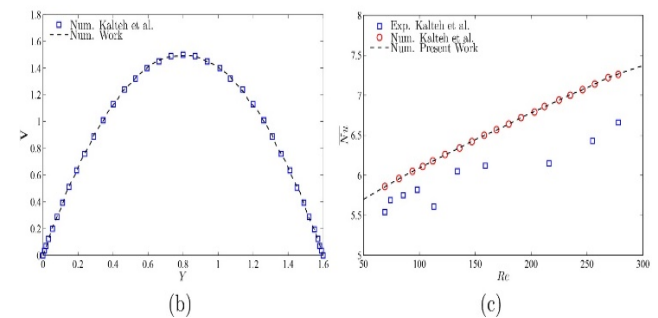


Fig 4. Comparisons of (a) dimensionless velocity profile of numerical results presented by Kalteh *et al.* (2012) and the current result; (b) average Nusselt number based on Re of the experimental and numerical results of Kalteh *et al.* (2012) and the current outcomes.

For the purpose of validation of the numerical code, it is imperative to carry out a comparison with the results that have been published previously. The results of the present work are compared with the experimental results of Chen and Wang (1998) with regard to flow and transfer of heat problem associated with forced convection in a 2D horizontal channel as shown in Fig. 3(a) and (b). In addition, the dimensionless velocity profile was compared with the numerical outcomes of Kalteh *et al.* (2012) and the average Nusselt number with Re of the experimental and numerical results of Kalteh *et al.* (2012), see Fig. 4(a) and (b). These results give assurance that the current numerical method is accurate.

4. Results and Discussion

Numerical results are provided in the current section regarding the velocity, streamlines and isotherms for three parameters: the Reynolds number ($10 \leq Re \leq 1000$), number of oscillations ($0 \leq N \leq 5$) and amplitude ($0.05 \leq A \leq 0.2$). The Prandtl number, length, height, width and inlet velocity are fixed

at $Pr = 4.623$, $W = 2$, $H = 0.2$, $D = 1$ and $U_{in} = 0.5$, respectively.

Fig. 5 and Fig. 6 illustrate the 3D velocity, streamlines and the isotherms as the Reynolds number (Re) is cahnged. With $Re = 100$, a laminar flow is observed, with the streamlines following the channel corrugation. With increasing Re , the flow close to the crests of the wall is distorted as a result of the greater inertial forces as well as higher velocity of flow in the channel center, causing the emergence of zones of recirculation close to the crests of the wall. As Re increases, recirculation intensity also increases; its highest level is reached at $Re = 1000$. Furthermore, the intensity of recirculation has a reduced value close to the upper wall in comparison to the lower wall, where the transfer of heat by convection plays a vital role. Based on the isotherms, the hot fluid occupies the bottom portion of the channel with respect to all Re values, but the cold fluid occupies the central and higher portions. Emergence of zones of recirculation at greater Re distorts the isotherms' shape, especially close to the crests of the undulated wall.

Figure 7 shows the dimensionless velocity, V , at the outlet boundary in addition to the local Nusselt number associated with the corrugated wall for different Re . In this case, V exhibits the same variation tendency for all Re values. Its value at the walls of the channel is zero as a result of the no-slip boundary condition, and it slowly rises to the maximal value close to the center. This maximal value rises with rising Re , thereby boosting the velocity of the entering flow. It is noteworthy that this is valid mostly in the center of the channel and towards the bottom wall and has a relationship with the flow isotherms as presented in Fig. 6. The Nusselt number exhibits recurring changes that follow the wavy wall; also, there is a considerable rise in its amplitude whenever Re is increased. This is an indication of an improvement in the rate of heat transfer over the heated wall with bigger Re . Actually, the emergence of zones of recirculation around the crests of the wall enhances mixing of fluid in that region and adds to the improvement in transfer of heat.

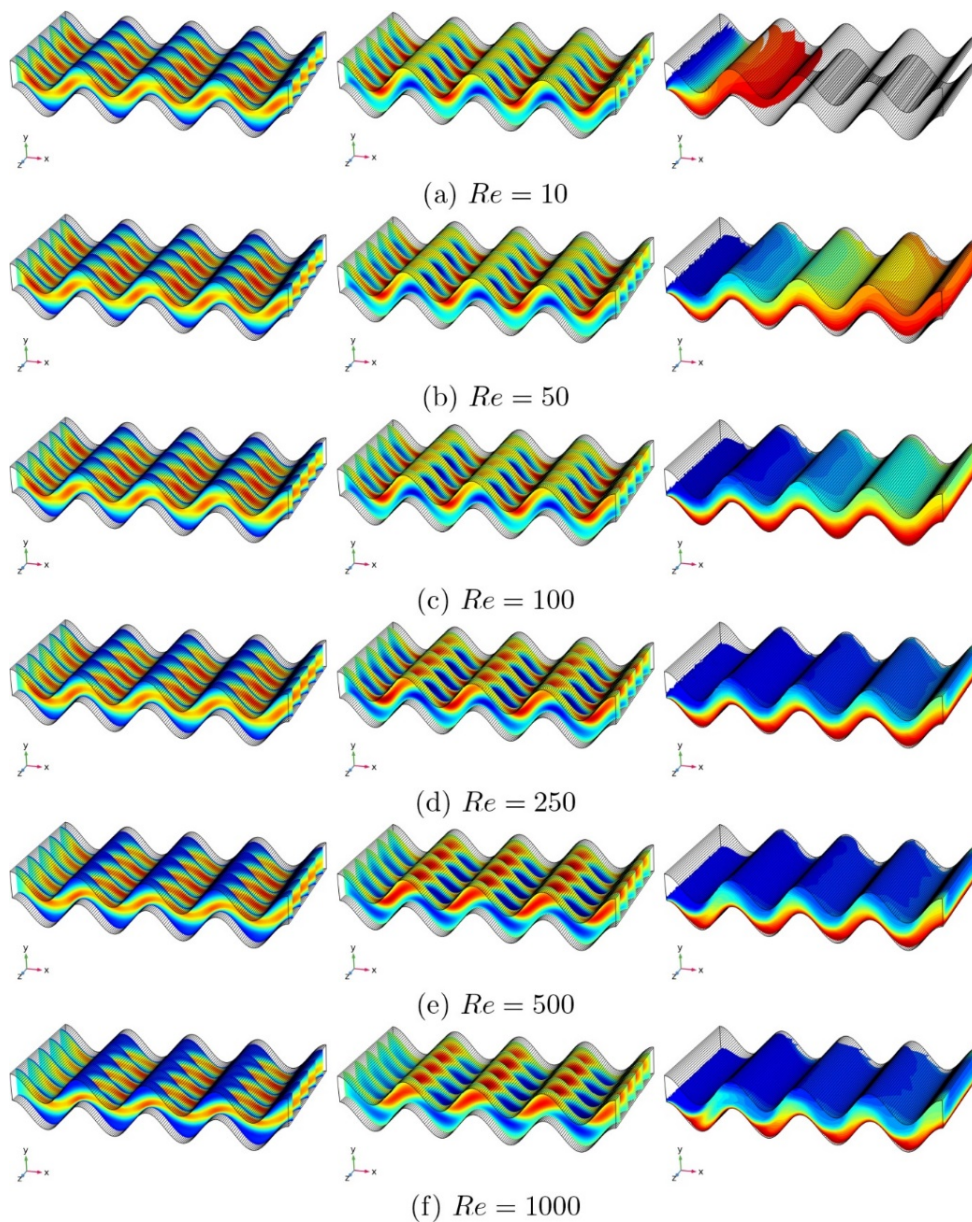


Fig 5. 3D variations of (left) velocity, (middle) streamlines, and (right) isotherms; evolution by Reynolds number (Re) for $N = 4$ and $A = 0.1$.

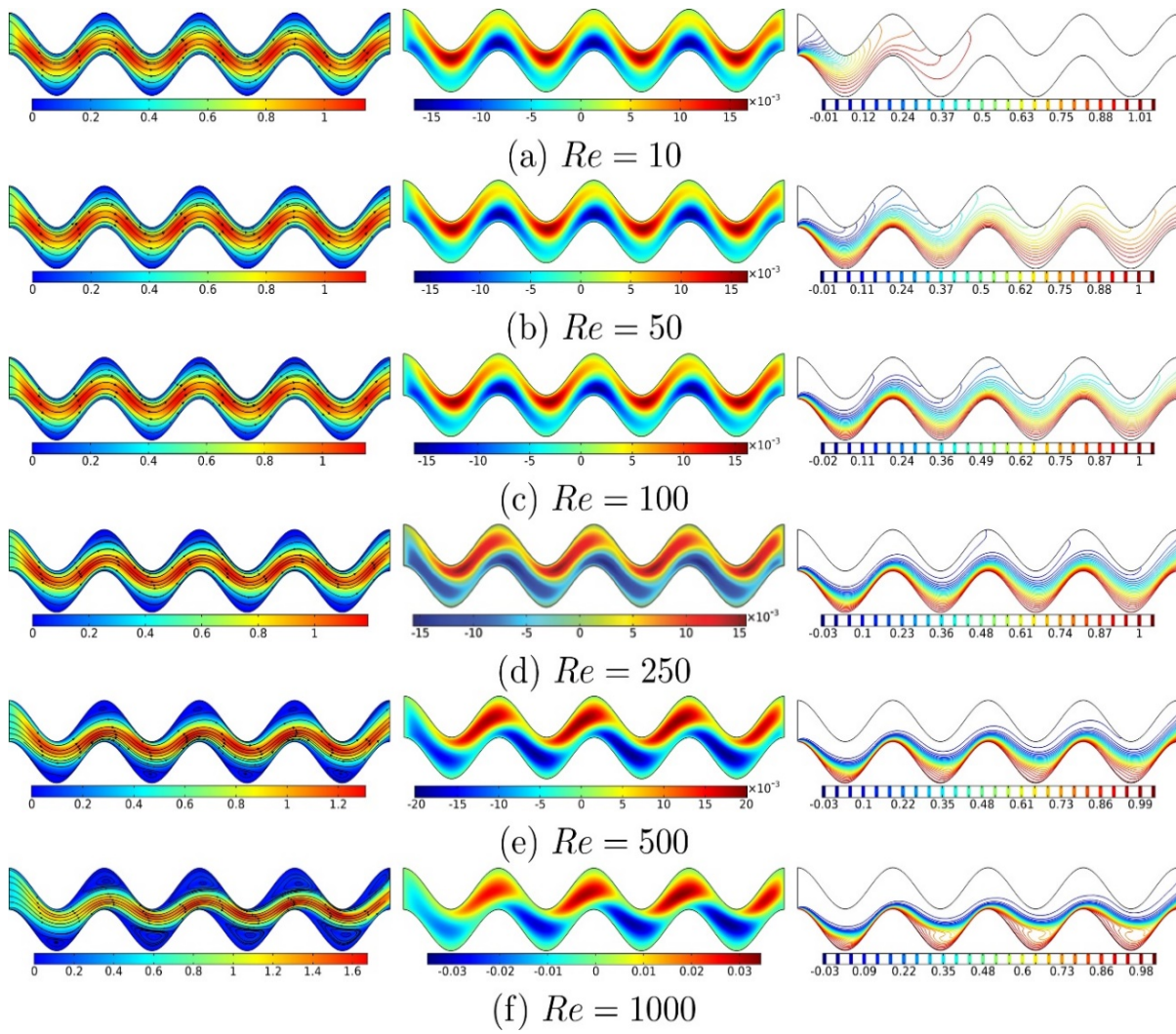


Fig 6. Continued in the plane (X, Y) .

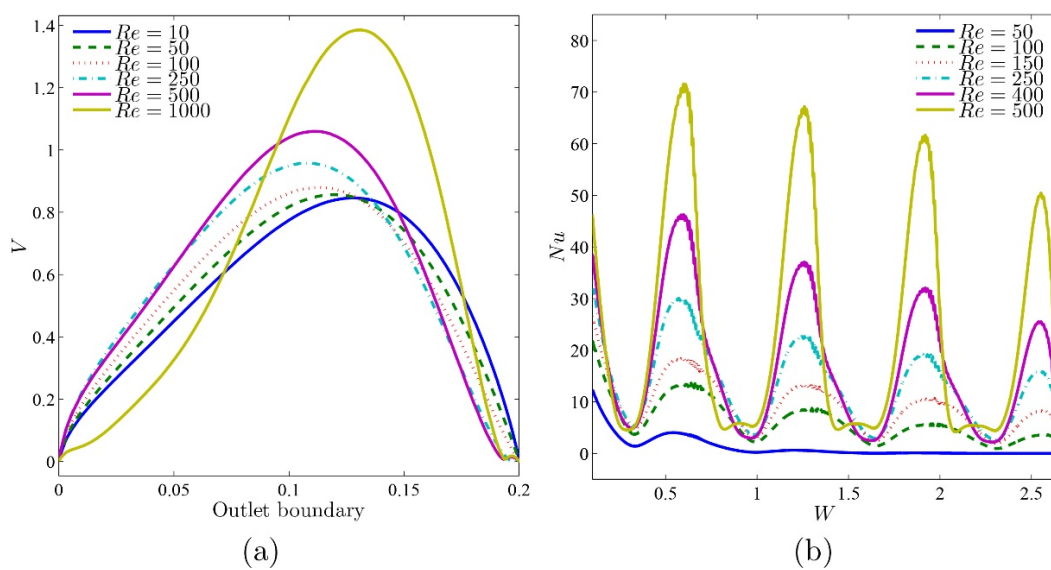


Fig 7. Changes associated with (a) non-dimensional velocity at the boundary of the outlet and (b) local Nusselt number interface based on W for various Re at $N = 4$ and $A = 0.1$.

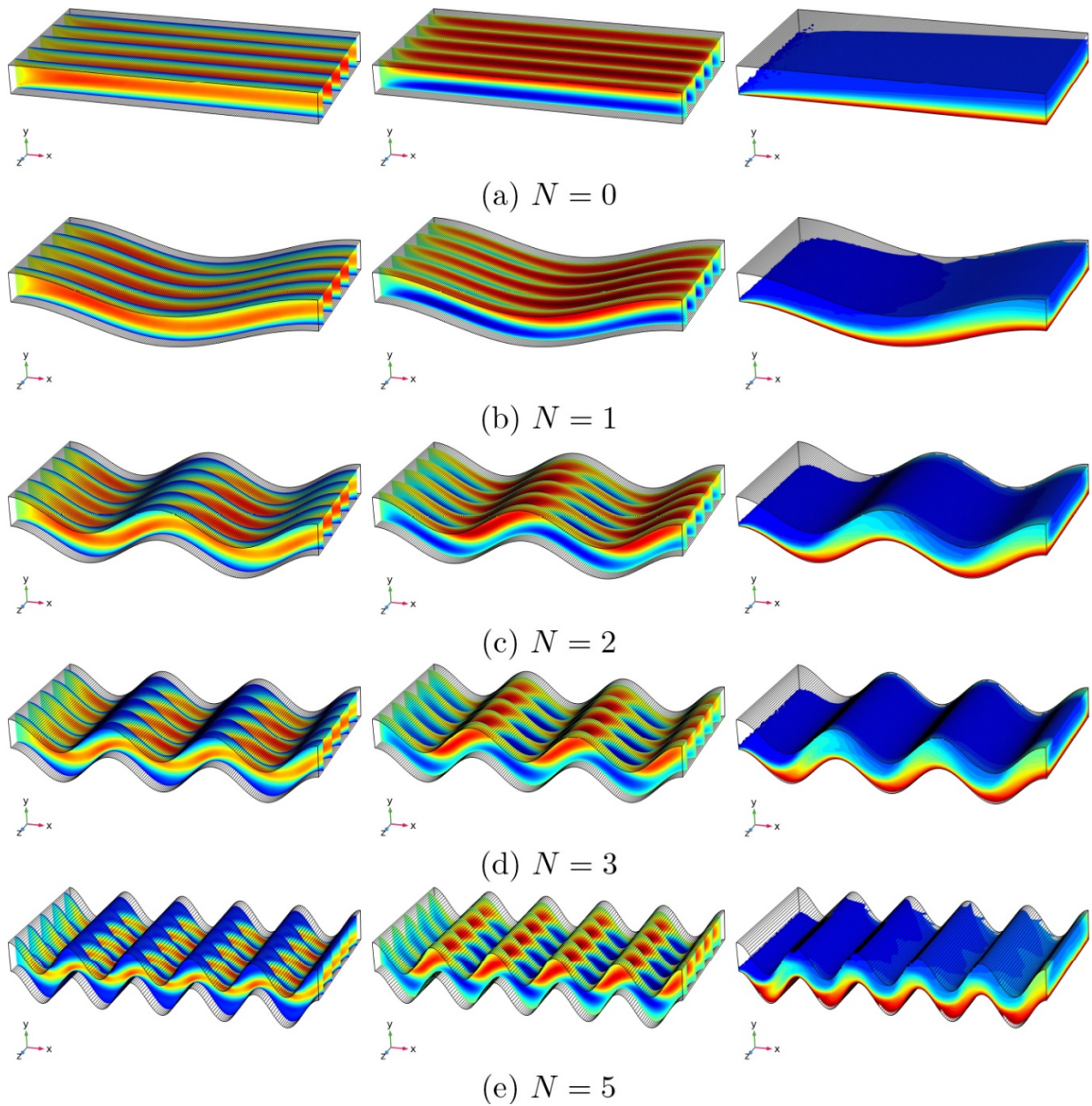


Fig 8. 3D changes associated with (left) velocity, (middle) streamlines, and (right) isotherms based on the number of oscillations (N) for $Re = 750$ and $A = 0.1$.

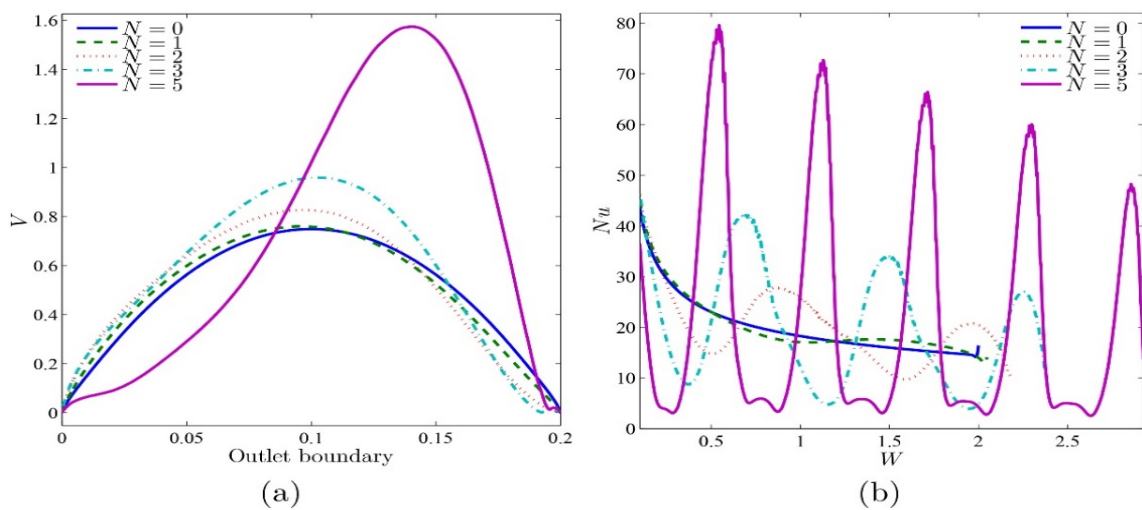


Fig 9. Changes associated with (a) non-dimensional velocity at the boundary of the outlet; (b) local Nusselt numbers interface based on W for various N at $Re = 750$ and $A = 0.1$.

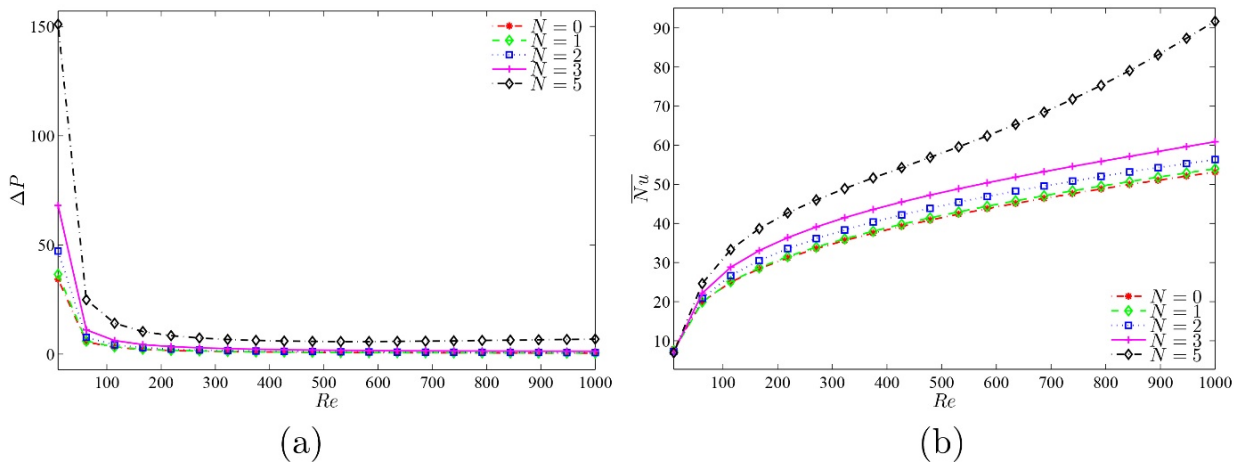


Fig 10. Changes associated with (a) pressure drop and (b) average Nusselt number based on Re for various N at $A = 0.1$.

Figure 8 presents the 3D velocity, streamlines and isotherms for various numbers of oscillations (N) for $Re = 750$ and $A = 0.1$. Regarding a channel that has straight walls, $N = 0$. In such a situation, the flow streamlines are symmetric straight lines around the center of the channel; this shows a small convective effect. With $N = 1$, an identical behavior is observed, which corresponds to a curved channel. However, with an increase beyond 2, the impact of N begins to materialize. Flow pattern is distorted by the wavy nature of the walls, and recirculation zones begin to emerge around the crests of the wall. The recirculation gets strengthened with increasing N (Al-Bonsrulahet al. 2021; Boonloi and Jedsadaratanachai 2015; Brodnianská and Kotšmid 2021). Notably, the distance between inlet and outlet remains unchanged, whereas the number of oscillations is raised. This points to a reduction in the wavelength of the walls. These walls have increased corrugation and lead to greater distortion of the flow field. In all cases, the isotherms exhibit identical behavior, the hot fluid is present at the channel bottom area and is crowded close to the bottom wall crests.

Figure 9 presents how N affects the dimensionless velocity (V) at the outlet boundary and the local Nusselt number (Nu) over the corrugated wall. With an increase in N , the maximal value of V rises, and the value is minimal when the channel walls are straight. Actually, with rising undulation of the walls at bigger N , the flow distortion caused by the undulated walls raises the discrepancy between the flow momentums of the channel center and walls, causing a greater velocity at the channel center. There is a significant rise in maximal Nu at bigger N values; this is as a result of the improved mixing in the zones of recirculation around the crests of the wall. Notwithstanding, there is a more rapid flow close to the troughs of the wall, and Nu has a minimal value in that area. This minimal value reduces with increased N . Generally, it seems that elevating N causes a little rise in the mean Nu .

Figure 10 depicts changes in the average Nusselt number (\bar{Nu}) and the pressure drop (Δp) for various Re values. In this regard, whenever there is an increment in Re , \bar{Nu} shows a higher value, which points to increased intensity in the transfer of heat, as a result of the intensified effects of inertial and the zones of recirculation around the hot corrugated wall. At the same time, it is evident that the pressure drop (Δp) decreases as N increases. Δp maintains a smaller value with higher Re

because of the higher fluid velocity. It is also clear that there is an effect of N on Δp only when Re is less than 100, while that effect disappears when the fluid velocity increases and the Re increases more than 100. Behaviors of the pressure drop, average Nusselt number and average skin friction factor with the governing parameters are presented in Fig. 10.

With regard to the evolution of vortices, Fig. 11 indicates that at lower amplitude, it is more definite and segregated. The 3-D plots in addition to the cross sectional view of the $X - Y$ plane with respect to the velocity streamlines, isotherms for different wave amplitudes (A) are given in Fig. 11. The numbers of waves (N) and Reynold's number (Re) are maintained respectively at 4 and 750. Based on Fig. 11 (first columns), it is observed that the streamlines are constituted of 4 pairs of powerful recirculation cells at the higher part, which occupies the major part of the domain, and 8 relatively less powerful cells at the bottom part of the domain for $A = 0.05$. As the wavelength is increased, the strength of the bottom-part vortices reduces and eventually disappears at $A = 0.125$. Nonetheless, the upper-portion vortices get bigger and stronger and cover the whole domain with increasing values of A . If the wave-amplitude is elevated, there is a rise in wavelength, causing a strong circulation of flow. Conclusively, the role played by the number of oscillations and wave amplitude in the transfer of heat along a corrugated surface is very important. With regard to the current wavy channel design, changes in number of oscillations and wave amplitude lower the fluid domain while increasing the surface area, thereby contributing to enhancement of heat transfer.

Figure 12 displays the changes of the dimensionless velocity interfaces with the boundary of the outlet and local Nusselt number interfaces with the bottom way surface for various amplitude (A) at $Re = 750$ and $N = 4$. The decrement in the coefficient of skin friction with Re is ascribed to the reduction of viscous force. The inverse relationship of the pressure drop and the Reynolds number is seen from Fig. 13.

Figure 14(a) and (b) explain the 3-D changes of average Nusselt number and average dimensionless temperature, respectively among N and A at $Re = 750$. The figure succinctly shows that heat transfer by convection rises when N and A are raised. Also, it is obvious that by raising N , there is an elevation of the averages of Nusselt number and dimensionless temperature.

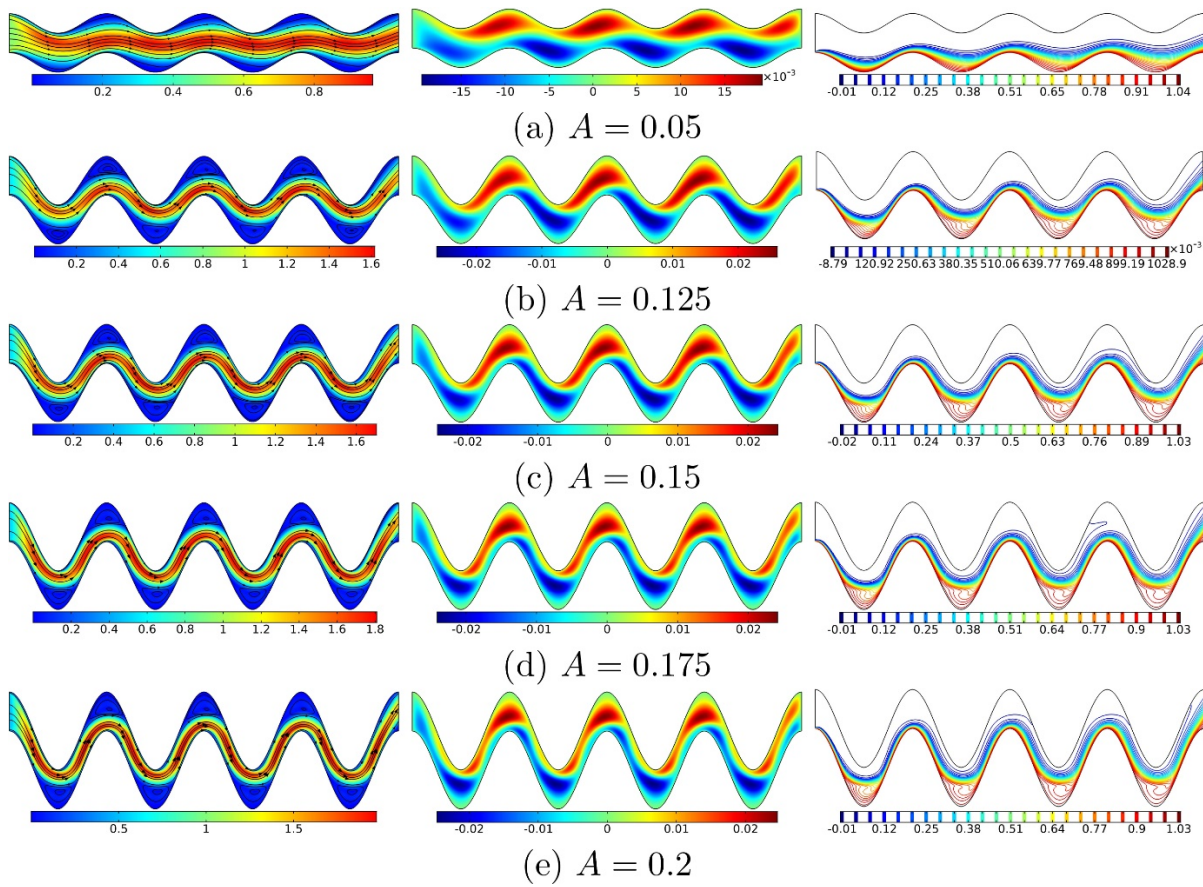


Fig 11 Changes associated with (left) velocity, (middle) streamlines, and (right) isotherms based on amplitude (A) with $Re = 750$ & $N = 4$ in the plane (X, Y).

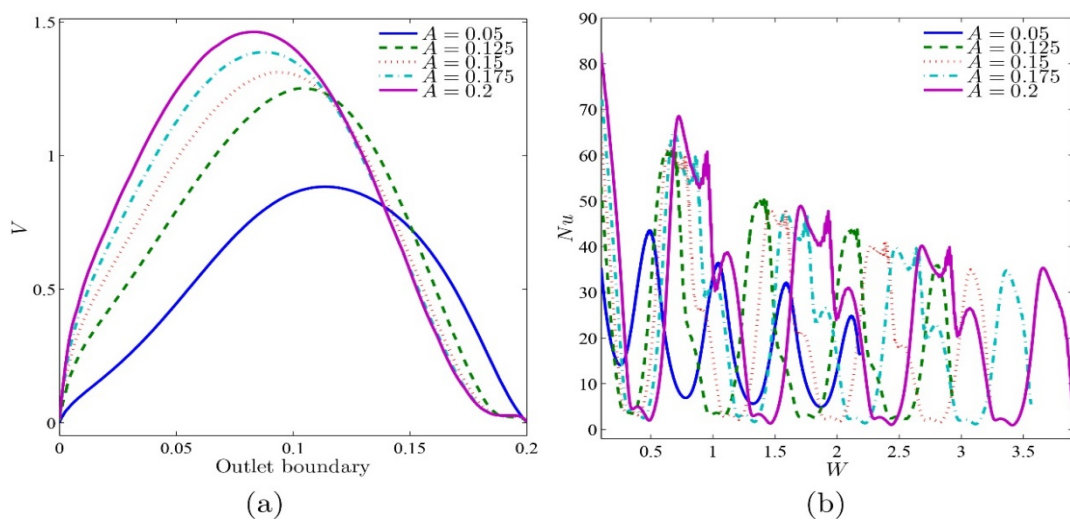


Fig 12. Changes associated with (a) non-dimensional velocity at the boundary of the outlet; (b) local Nusselt numbers interface based on W for various A at $Re = 750$ and $N = 4$.

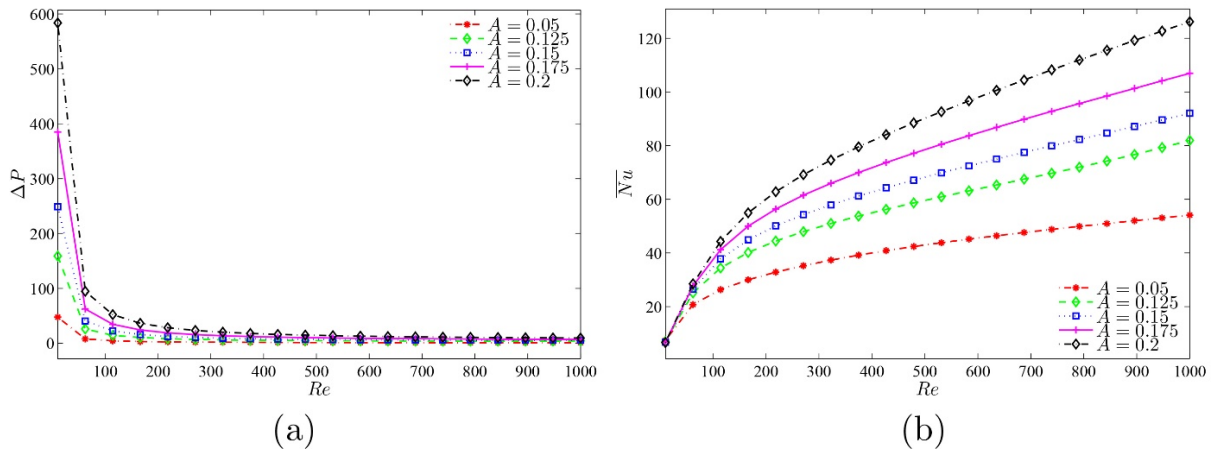


Fig 13. Variations of (a) pressure drop; (b) average Nusselt number based on Re with various A at $N = 4$.

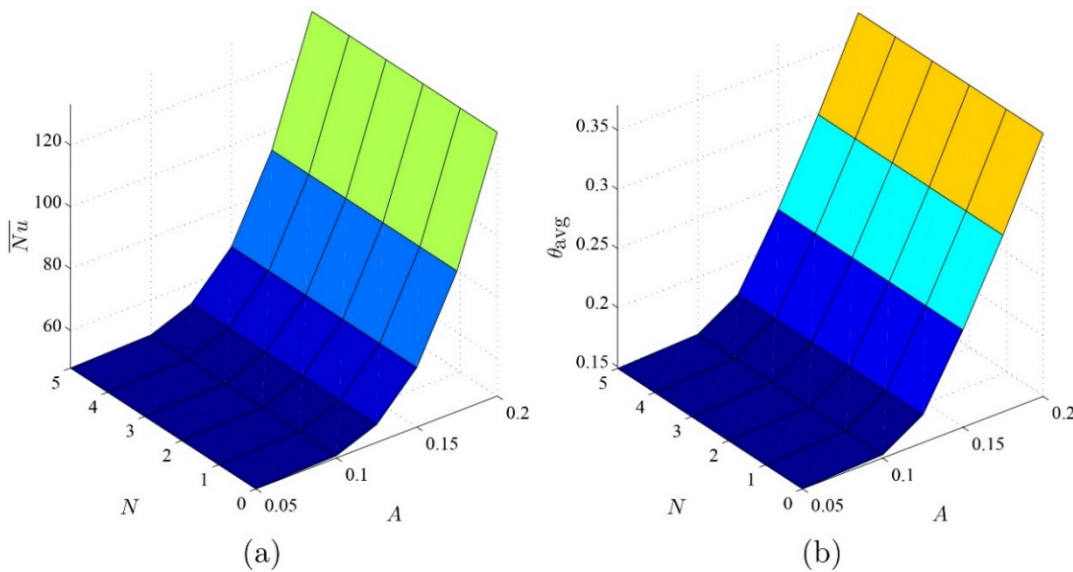


Fig 14. 3D Changes associated with (a) average Nusselt number; (b) average dimensionless temperature based on N and A at $Re = 750$.

5. Conclusions

This study was performed numerically regarding the transfer of heat based on forced convection under laminar flow condition in a corrugated-channel to analyze the impacts of the Reynolds number, number of oscillations and amplitude of the wall on heat transfer. Whenever there is an increase in the Reynolds number, the average Nusselt number is elevated, which is indicative of heat transfer of greater intensity. The flow pattern is distorted by the undulations of the walls, and recirculation zones begin to emerge around the crests of the walls. With an increment in number of oscillations, the maximal value of the average velocity is elevated, and its minimal value occurs when the channel walls are straight. The rate of heat transfer increases about 0.28% with the rise of the number of oscillation and for low Reynolds number. While for high Reynolds number, the rate of heat transfer increases about 0.41% with rising of the number of oscillations. Regarding the current design of the wavy channel, changes in number of oscillations and wave amplitude lower the fluid domain while increasing the surface area, thereby contributing to the enhancement of heat transfer. A rise of the wall amplitude improves the rate of heat transfer about 0.91% when the Reynolds number is equal 100. In addition,

when the Reynolds number is equal 500, the rate of heat transfer grows about 1.1% with the increase of the wall amplitude.

Acknowledgments

The work was supported by the Universiti Kebangsaan Malaysia (UKM) research grant GP-2021-K006388. We thank the respected reviewers for their constructive comments which clearly enhanced the quality of the manuscript.

References

Abd Rahim, A. T., & Hilo, A. K. (2021). Fluid flow and heat transfer over corrugated backward facing step channel. *Case Studies in Thermal Engineering*, 24, 100862. <https://doi.org/10.1016/j.csite.2021.100862>

Adhikari, R. C., Wood, D. H., & Pahlevani, M. (2020). An experimental and numerical study of forced convection heat transfer from rectangular fins at low Reynolds numbers. *International Journal of Heat and Mass Transfer*, 163, 120418. <https://doi.org/10.1016/j.ijheatmasstransfer.2020.120418>

AL-bonsrulah, H. A., Alshukri, M. J., Mikhaeel, L. M., AL-sawaf, N. N., Nesrine, K., Reddy, M. V., & Zaghbi, K. (2021). Design and simulation studies of hybrid power systems based on photovoltaic,

- wind, electrolyzer, and pem fuel cells. *Energies*, 14(9), 2643. <https://doi.org/10.3390/en14092643>
- AL-bonsrulah, H. A., Alshukri, M. J., Alsabery, A. I., & Hashim, I. (2021). Numerical and theoretical study of performance and mechanical behavior of PEM-FC using innovative channel geometrical configurations. *Applied Sciences*, 11(12), 5597. <https://doi.org/10.3390/app11125597>
- Ali, S., Eidan, A., Al-Sahlan, A., Alshukri, M., & Ahmad, A. (2020). The Effect of vibration pulses on the thermal performance of evacuated tube heat pipe solar collector. *Journal of Mechanical Engineering Research and Developments*, 43, 340.
- Alsabery, A. I., Hajjar, A., Sheremet, M. A., Ghalambaz, M., & Hashim, I. (2021). Impact of particles tracking model of nanofluid on forced convection heat transfer within a wavy horizontal channel. *International Communications in Heat and Mass Transfer*, 122, 105176. <https://doi.org/10.1016/j.icheatmasstransfer.2021.105176>
- Alsabery, A. I., Parvin, S., Ghalambaz, M., Chamkha, A. J., & Hashim, I. (2020). Convection heat transfer in 3D wavy direct absorber solar collector based on two-phase nanofluid approach. *Applied Sciences*, 10(20), 7265. <https://doi.org/10.3390/app10207265>
- Alsabery, A. I., Sidik, N. A. C., Hashim, I., & Muhammad, N. M. (2022). Impacts of two-phase nanofluid approach toward forced convection heat transfer within a 3D wavy horizontal channel. *Chinese Journal of Physics*, 77, 350-365. <https://doi.org/10.1016/j.cjph.2021.10.049>
- Alshukri, M. J., Eidan, A. A., & Najim, S. I. (2021). The influence of integrated Micro-ZnO and Nano-CuO particles/paraffin wax as a thermal booster on the performance of heat pipe evacuated solar tube collector. *Journal of Energy Storage*, 37, 102506. <https://doi.org/10.1016/j.est.2021.102506>
- Alshukri, M. J., Hussein, A. K., Eidan, A. A., & Alsabery, A. I. (2022). A review on applications and techniques of improving the performance of heat pipe-solar collector systems. *Solar Energy*, 236, 417-433. <https://doi.org/10.1016/j.solener.2022.03.022>
- ALshukri, M. J., Madloul, N. A., & Jabbar, N. A. (2018). Improving heat transfer by employing fin array of various innovative shapes in natural convection. *International Journal of Mechanical & Mechatronics Engineering*, 18(1), 98-105
- Boonloi, A., & Jedsadaratanachai, W. (2015). Turbulent forced convection in a heat exchanger square channel with wavy-ribs vortex generator. *Chinese Journal of Chemical Engineering*, 23(8), 1256-1265. <https://doi.org/10.1016/j.cjche.2015.04.001>
- Bourouis, M., & Prévost, M. (1994). Etude numérique de la structure de l'écoulement, en régime laminaire, dans une conduite pleine à paroi ondulée. *The Chemical Engineering Journal and the Biochemical Engineering Journal*, 55(1-2), 15-25. [https://doi.org/10.1016/0923-0467\(94\)87002-0](https://doi.org/10.1016/0923-0467(94)87002-0)
- Brodnianská, Z., & Kotšmid, S. (2021). Intensification of convective heat transfer in new shaped wavy channel configurations. *International Journal of Thermal Sciences*, 162, 106794. <https://doi.org/10.1016/j.ijthermalsci.2020.106794>
- Chen, Y. M., & Wang, K. C. (1998). Experimental study on the forced convective flow in a channel with heated blocks in tandem. *Experimental Thermal and Fluid Science*, 16(4), 286-298. [https://doi.org/10.1016/S0894-1777\(97\)10033-4](https://doi.org/10.1016/S0894-1777(97)10033-4)
- Durgam, S., Venkateshan, S. P., & Sundararajan, T. (2017). Experimental and numerical investigations on optimal distribution of heat source array under natural and forced convection in a horizontal channel. *International Journal of Thermal Sciences*, 115, 125-138. <https://doi.org/10.1016/j.ijthermalsci.2017.01.017>
- Eidan, A. A., Alshukri, M. J., Al-fahham, M., AlSahlani, A., & Abduridha, D. M. (2021). Optimizing the performance of the air conditioning system using an innovative heat pipe heat exchanger. *Case Studies in Thermal Engineering*, 26, 101075. <https://doi.org/10.1016/j.csite.2021.101075>
- Errico, O., & Stalio, E. (2014). Direct numerical simulation of turbulent forced convection in a wavy channel at low and order one Prandtl number. *International Journal of Thermal Sciences*, 86, 374-386. <https://doi.org/10.1016/j.ijthermalsci.2014.07.021>
- Feijó, B. C., Lorenzini, G., Isoldi, L. A., Rocha, L. A. O., Goulart, J. N. V., & Dos Santos, E. D. (2018). Constructal design of forced convective flows in channels with two alternated rectangular heated bodies. *International Journal of Heat and Mass Transfer*, 125, 710-721. <https://doi.org/10.1016/j.ijheatmasstransfer.2018.04.086>
- Hajjalilababaei, M., & Saghir, M. Z. (2022). A critical review of the straight and wavy microchannel heat sink and the application in lithium-ion battery thermal management. *International Journal of Thermofluids*, 100153. <https://doi.org/10.1016/j.ijft.2022.100153>
- Izumi, R., Yamashita, H., Oyakawa, K., & Mori, N. (1983). Fluid Flow and Heat Transfer in Corrugated Wall Channels : 3rd Report, Effects of Bending Angles in the Case Where Channels Are Bent Two Times. *Bulletin of JSME*, 26(216): 1027-35. <https://doi.org/10.1299/jsme1958.26.1146>
- Jabbar, N. A., ALshukri, M. J., Rasheed, W. A., & Hussain, I. Y. (2018). Numerical investigation of new cooling method for clinker flow in parallel with Air flow at different height ratios. *International Journal of Mechanical & Mechatronics Engineering*, 18(3):1-17. <https://doi.org/10.4028/www.scientific.net/KEM.895.157>
- Jing, D., Song, J., & Sui, Y. I. (2020). Hydraulic and thermal performances of laminar flow in fractal treelike branching microchannel network with wall velocity slip. *Fractals*, 28(02), 2050022. <https://doi.org/10.1142/S0218348X2050022X>
- Kalteh, M., Abbassi, A., Saffar-Avval, M., Frijns, A., Darhuber, A., & Harting, J. (2012). Experimental and numerical investigation of nanofluid forced convection inside a wide microchannel heat sink. *Applied Thermal Engineering*, 36, 260-268. <https://doi.org/10.1016/j.applthermaleng.2011.10.023>
- Kim, S. M., & Mudawar, I. (2013). Universal approach to predicting heat transfer coefficient for condensing mini/micro-channel flow. *International Journal of Heat and Mass Transfer*, 56(1-2), 238-250. <https://doi.org/10.1016/j.ijheatmasstransfer.2012.09.032>
- Kumar, R., Tiwary, B., & Singh, P. K. (2022). Thermofluidic analysis of Al₂O₃-water nanofluid cooled branched wavy heat sink. *Applied Thermal Engineering*, 201, 117787. <https://doi.org/10.1016/j.applthermaleng.2021.117787>
- Leontini, J. S., Thompson, M. C., & Hourigan, K. (2007). Three-dimensional transition in the wake of a transversely oscillating cylinder. *Journal of Fluid Mechanics*, 577, 79-104. <https://doi.org/10.1017/S0022112006004320>
- Li, X. J., Zhang, J. Z., Tan, X. M., & Wang, Y. (2022). Enhancing forced-convection heat transfer of a channel surface with piezo-fans. *International Journal of Mechanical & Mechatronics Engineering*, 107437. <https://doi.org/10.1016/j.ijmecsci.2022.107437>
- Lyu, Z., Pourfatah, F., Arani, A. A. A., Asadi, A., & Foong, L. K. (2020). On the thermal performance of a fractal microchannel subjected to water and kerosene carbon nanotube nanofluid. *Scientific Reports*, 10(1), 1-16. <https://doi.org/10.1038/s41598-020-64142-w>
- Mehta, S. K., Pati, S., & Baranyi, L. (2022). Effect of amplitude of walls on thermal and hydrodynamic characteristics of laminar flow through an asymmetric wavy channel. *Case Studies in Thermal Engineering*, 31, 101796. <https://doi.org/10.1016/j.csite.2022.101796>
- Miroshnichenko, I. V., Sheremet, M. A., Pop, I., & Ishak, A. (2017). Convective heat transfer of micropolar fluid in a horizontal wavy channel under the local heating. *International Journal of Mechanical Sciences*, 128, 541-549. <https://doi.org/10.1016/j.ijmecsci.2017.05.013>
- Ra, N. (2022). Performance improvement of rectangular microchannel heat sinks using nanofluids and wavy channels. *Numerical Heat Transfer, Part A: Applications*, 82(10), 619-639. <https://doi.org/10.1080/10407782.2022.2083840>
- Nishimura, T., Arakawa, S., Murakami, S., & Kawamura, Y. (1989). Oscillatory viscous flow in symmetric wavy-walled channels. *Chemical Engineering Science*, 44(10), 2137-2148. [https://doi.org/10.1016/0009-2509\(89\)85148-6](https://doi.org/10.1016/0009-2509(89)85148-6)
- Nishimura, T., Murakami, S., & Kawamura, Y. (1993). Mass transfer in a symmetric sinusoidal wavy-walled channel for oscillatory flow. *Chemical Engineering Science*, 48(10), 1793-1800. [https://doi.org/10.1016/0009-2509\(93\)80349-U](https://doi.org/10.1016/0009-2509(93)80349-U)
- Rush, T. A., Newell, T. A., & Jacobi, A. M. (1999). An experimental study of flow and heat transfer in sinusoidal wavy passages. *International Journal of Heat and Mass Transfer*, 42(9), 1541-1553. [https://doi.org/10.1016/S0017-9310\(98\)00264-6](https://doi.org/10.1016/S0017-9310(98)00264-6)
- Sheikholeslami, M. (2022). Numerical analysis of solar energy storage within a double pipe utilizing nanoparticles for expedition of melting. *Solar Energy Materials and Solar Cells*, 245, 111856. <https://doi.org/10.1016/j.solmat.2022.111856>
- Sheikholeslami, M. (2022b). Numerical investigation of solar system equipped with innovative turbulator and hybrid nanofluid. *Solar Energy Materials and Solar Cells*, 243, 111786. <https://doi.org/10.1016/j.solmat.2022.111786>

- Sheikholeslami, M., & Ebrahimpour, Z. (2022). Thermal improvement of linear Fresnel solar system utilizing Al_2O_3 -water nanofluid and multi-way twisted tape. *International Journal of Thermal Sciences*, 176, 107505. <https://doi.org/10.1016/j.ijthermalsci.2022.107505>
- Sheikholeslami, M., Said, Z., & Jafaryar, M. (2022). Hydrothermal analysis for a parabolic solar unit with wavy absorber pipe and nanofluid. *Renewable Energy*, 188, 922-932. <https://doi.org/10.1016/j.renene.2022.02.086>
- Vasudeviah, M., & Balamurugan, K. (2001). On forced convective heat transfer for a Stokes flow in a wavy channel. *International Communications in Heat and Mass Transfer*, 28(2), 289-297. [https://doi.org/10.1016/S0735-1933\(01\)00235-4](https://doi.org/10.1016/S0735-1933(01)00235-4)
- Wang, G. V., & Vanka, S. P. (1995). Convective heat transfer in periodic wavy passages. *International Journal of Heat and Mass Transfer*, 38(17), 3219-3230. [https://doi.org/10.1016/0017-9310\(95\)00051-A](https://doi.org/10.1016/0017-9310(95)00051-A)



© 2023. The Author(s). This article is an open access article distributed under the terms and conditions of the Creative Commons Attribution-ShareAlike 4.0 (CC BY-SA) International License (<http://creativecommons.org/licenses/by-sa/4.0/>)